

# Synergistic Inhibition Effect of 3-Carboxypyridine and Potassium Iodide on Mild Steel Corrosion in H<sub>2</sub>SO<sub>4</sub>: Electrochemical and Surface Analyses

Neelu Dheer<sup>1</sup>, Amarpreet K. Kalra<sup>2</sup>, Darshan Singh<sup>3</sup>, Sanjeev Kumar Ujjain<sup>4</sup>, Preety Ahuja<sup>4</sup>, Gurmeet Singh<sup>5</sup>, M. Ramananda Singh<sup>6\*</sup> and Rajni Kanojia<sup>7\*</sup>

<sup>1</sup>Department of Chemistry, Acharya Narendra Dev College, University of Delhi, Delhi 110019, India

<sup>2</sup>Department of Chemistry, SGTB Khalsa College, University of Delhi, Delhi 110007, India

<sup>3</sup>Department of Chemistry, Daulat Ram College, University of Delhi, Delhi 110007, India

<sup>4</sup>Research Initiative for Supra-Materials, Shinshu University, Nagano-city, Japan

<sup>5</sup>Department of Chemistry, University of Delhi, Delhi, India

<sup>6</sup>Department of Chemistry, Kirori Mal College, University of Delhi, Delhi 110007, India

<sup>7</sup>Department of Chemistry, Shivaji College, University of Delhi, Delhi 110027, India

\*Corresponding authors: drrajnikanojia@gmail.com, rajnikanojia@shivaji.du.ac.in, rsingh@kmc.du.ac.in

Received 09/05/2022; accepted 09/08/2022

<https://doi.org/10.4152/pea.2024420104>

---

## Abstract

The effective inhibition of MS corrosion in H<sub>2</sub>SO<sub>4</sub> by CP and CP + KI was assessed by EIS. SM of MS was studied using SEM and AFM. The rise in R<sub>ct</sub> and decrease in C<sub>dl</sub>, with higher C of CP and CP + KI, confirmed MS CI. IE(%) increased with higher C of CP only and CP + KI (from 10<sup>-3</sup> to 10<sup>-1</sup> M). CP maximum IE(%) was 93.9%, at 10<sup>-1</sup> M. CP + KI, due to I<sup>-</sup> ions synergistic effect, showed an IE(%) of about 98.8%, at 10<sup>-1</sup> M. CP only and CP + KI adsorption mechanism followed Langmuir's isotherm. SM studies suggested that a barrier film of CP only and CP + KI, mitigated MS surface corrosion. CP + KI is an efficient inhibitor in H<sub>2</sub>SO<sub>4</sub>.

**Keywords:** AFM; corrosion; CP; EIS; IE(%); KI; MS; SM; SEM.

---

## Introduction\*

Metallic corrosion is affected by environmental factors (including moisture and T) and surface conditions, such as energy, exposed area, roughness and oxides stability, which are inherently related to the materials composition. Unanticipated failures (stream generator and pipeline stress corrosion cracking) and system shutdowns occur in oil and gas industries, at pipelines, liquefied natural gas terminals and refineries, due to corrosion, which results in monetary losses. When analyzing any method to control corrosion in industrial systems, operational processes should

---

\* The abbreviations and symbols definition lists are in page 67.

comprise factors such as coatings durability, maintenance schedule, service life, sustainability and life cycle costs.

The selection of the most effective corrosion control system is important. Corrosion protection systems include galvanizing, painting, coating, and the use of CI, such as organic, inorganic, volatile, adsorption-type, anodic, cathodic, mixed and environmental friendly inhibitors. CI performance is mainly related to the molecules physicochemical properties, such as their electronic structure, electron density at the donor atom and functional group. Pyridine and its derivatives are classified as accepted CI. The influence of numerous functional groups on pyridine, and their derivatives, capability as CI for various metals and alloys in acidic/alkaline media, has been reported in literature [1-12]. The heterocyclic compound is adsorbed onto the metallic surface through their active sites. The inhibitor adsorbed protective layers shield the metallic surface from direct contact with corrosive ions [13-23].

The present paper studied the CI of MS in  $H_2SO_4$  by CP only and CP + KI, employing Ec methods such as EIS. It discussed the complex-plane impedance Nyquist and Bode plots for MS in 0.5 M  $H_2SO_4$ , without and with different C of CP, and it also described KI synergistic effect, at 308 K. SEM and AFM techniques were used to analyze the SM of MS.

## **Experimental analysis**

### ***Specimen preparation***

Uniform surfaces of MS specimens were prepared with a grinding machine using emery paper of different grades (220, 400, 800 and 1000). MS was employed as WE. For the EIS experiment, the WE exposed area was of 1 cm<sup>2</sup>.

### ***Ec technique***

Ec investigations were done by an CHI 760D model Ec work station. EIS experiment was performed with an AC signal of 1 mV amplitude, at OCP, and at a frequency range from 100 KHz to 10 MHz.

### ***SM***

The SM of MS coupons was studied using a Ziess S-3700 N SEM and Nanosurf Naio AFM (both from Germany). The MS surface area of 1 cm<sup>2</sup> was smoothed with 150, 600 and 2000 grade emery paper, and then cleaned with distilled water and acetone. MS was exposed to  $H_2SO_4$  without and with 10<sup>-1</sup> M CP only and CP + KI, at 298 K, for 6 h, and then it was washed and dried before surface examinations.

## **Results and discussion**

### ***EIS***

The CI of MS was investigated by EIS method. Fig. 1 shows impedance plots for MS in  $H_2SO_4$  without and with CP only and CP + KI, at 308 K. Nyquist plots show that the depressed semi-circle increased with higher C of CP, indicating that MS corrosion was largely controlled by a charge transfer mechanism. This kind of

behavior is a common feature of solid electrodes, which causes frequency dispersion, roughness and inhomogeneities on the solid electrode surface.

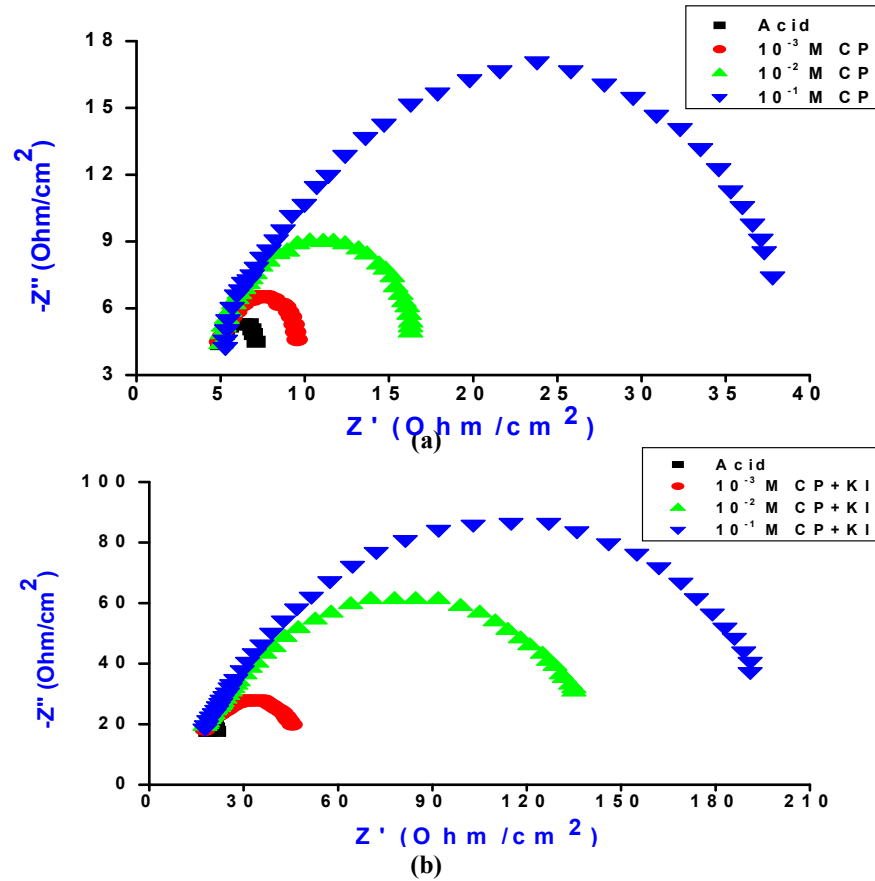


**Figure 1:** Nyquist Plots of MS in 0.5 M H<sub>2</sub>SO<sub>4</sub>, at 308 K, with various C of: (a) CP; and (b) CP + KI.

EIS parameters, such as  $R_{ct}$ ,  $C_{dl}$  and  $IE(\%)$ , are shown in Table 1.  $IE(\%)$  was evaluated by using the following relation [24]:

$$IE\% = \frac{R_{ct} - R_{ct}^0}{R_{ct}} \times 100 \quad (1)$$

where  $R_{ct}^0$  denotes  $R_{ct}$  of the solution without inhibitor.  $C_{dl}$  was determined from the equation given below:

$$C_{dl} = (2\pi f R_{ct})^{-1} \quad (2)$$

The Bode plot (Fig. 2 a-d) shows that  $\theta_{max}$  values are related to the electrode  $\eta$ . Low  $\theta_{max}$  values correspond to high  $\eta$ . Table 1 shows that  $\theta_{max}$  in H<sub>2</sub>OS<sub>4</sub> was about 26.3, and it gradually increased upon CP + KI addition, which suggests that  $\eta$  decreased with the inhibitor.  $\theta_{max}$  observed upon I ions addition indicates that the system was approaching an ideal polarized electrode.

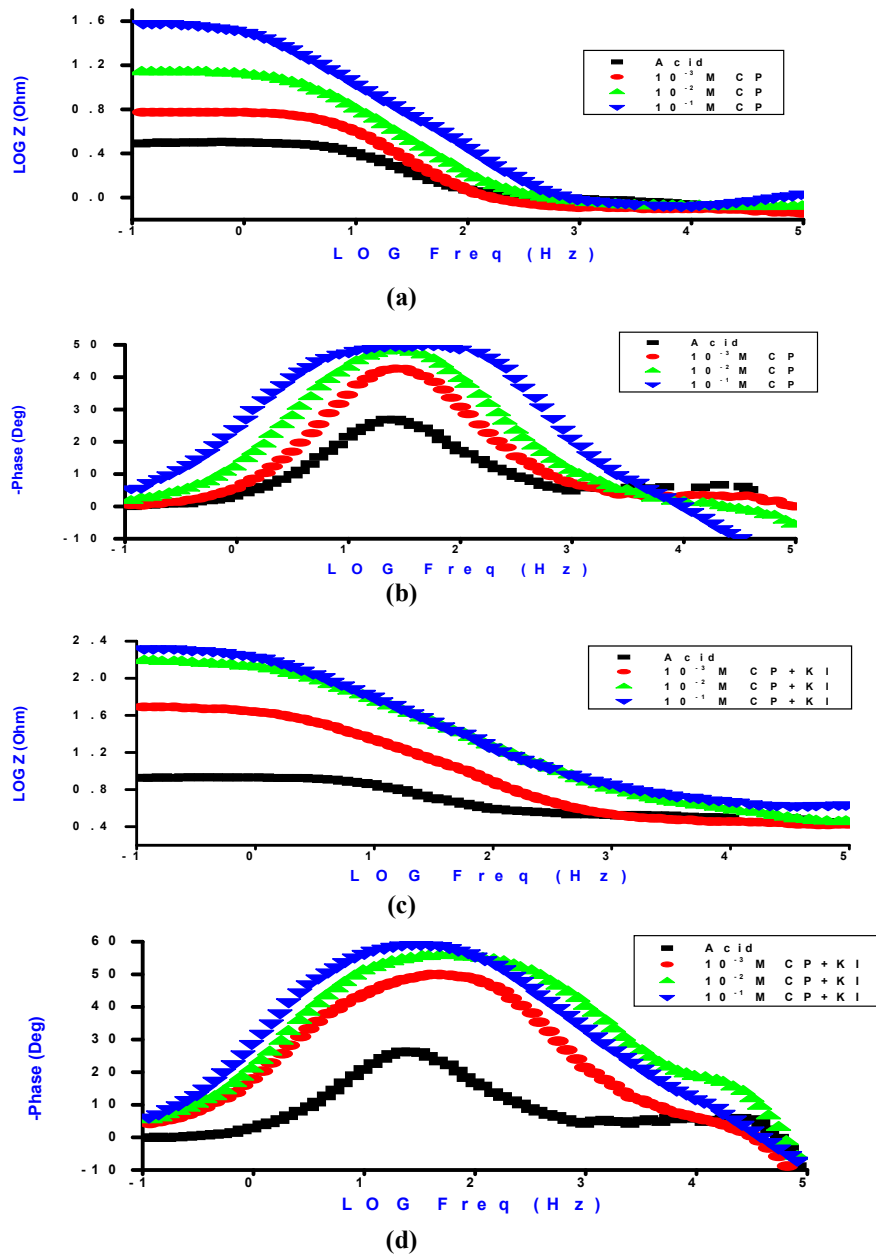


**Figure 2:** Bode plots of MS in 0.5 M H<sub>2</sub>SO<sub>4</sub>, at 308 K, with various C of: (a) and (b) CP; (c) and (d) CP + KI.

**Table 1:** Demonstration of EIS data on MS with various C of CP and CP + KI in 0.5 M H<sub>2</sub>SO<sub>4</sub>.

Additive	C (M)	R <sub>ct</sub> (Ω/cm <sup>2</sup> )	Freq. (Hz)	C <sub>dl</sub> (F/cm <sup>2</sup> ) x 10 <sup>-4</sup>	IE(%)	θ	θ <sub>max</sub>
H <sub>2</sub> SO <sub>4</sub>	0	2.404	11.91	55.62	-	-	26.3
	10 <sup>-1</sup>	39.561	1.738	2.316	93.92	0.939	49.1
CP	10 <sup>-2</sup>	13.192	4.542	2.658	81.77	0.817	47.6
	10 <sup>-3</sup>	5.156	8.071	3.826	53.37	0.533	42.3
CP + KI	10 <sup>-1</sup>	206.179	1.43	5.39	98.83	0.988	59.3
	10 <sup>-2</sup>	142.461	2.55	4.38	98.31	0.983	55.8
	10 <sup>-3</sup>	32.315	2.55	19.32	92.56	0.925	49.9

Table 1 reveals that there was increase in  $R_{ct}$  value with higher C of CP, from  $10^{-3}$  to  $10^{-1}$  M (Fig. 3). In contrast, there was a decrease in  $C_{dl}$  value with higher C of CP. Due to the synergistic effect of I ions and the rise in the inhibitor C, the interface Rp increased, because of CP + KI molecules adsorption onto the MS surface. The  $\theta$  by CP and CP + KI molecules allowed for CI [25]. The following equation shows the correlation between  $C_{dl}$  and the protective layer thickness.

$$\delta_{org} = \frac{\epsilon_0 \epsilon_t}{C_{dl}} \quad (3)$$

where  $\epsilon_0$  and  $\epsilon_t$  denote vacuum and relative dielectric constants, respectively.  $C_{dl}$  values were reduced, due to a decrease in the local dielectric constant or to an increase in the electrical double layer, caused by CP molecules adsorption onto the metal/solution interface, and by the water molecules gradual replacement by the inhibitor on the MS surface. This resulted in lower MS dissolution [26], confirming that CP effectively retarded MS corrosion process in  $H_2OS_4$ .

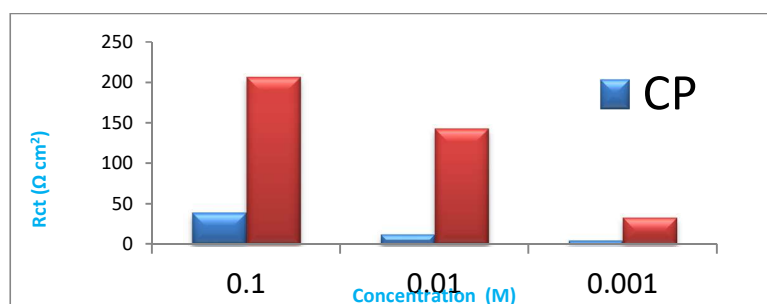


Figure 3: Variation of  $R_{ct}$  with CP and CP + KI C.

Fig. 4 shows the relation between IE(%) of CP and  $\log C$ , at 308 K, and that IE(%) increased with higher C of CP and CP + KI, from  $10^{-3}$  to  $10^{-1}$  M.

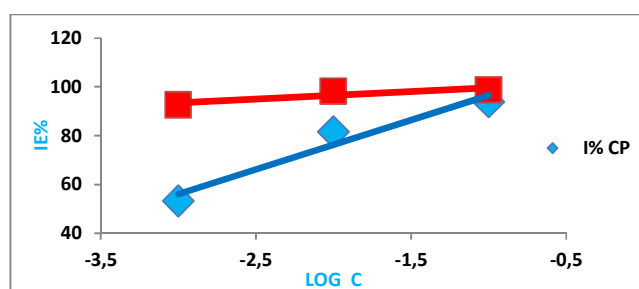


Figure 4: IE (%) versus  $\log C$ .

CP IE(%) values were 53.3, 81.7 and 93.9%, at  $10^{-3}$ ,  $10^{-2}$  and  $10^{-1}$  M, respectively. However, they were 92.5, 98.3 and 98.8%, at  $10^{-3}$ ,  $10^{-2}$  and  $10^{-1}$  M, respectively, upon I ions addition, accordingly [27, 28]. Due to I ions large ionic radius and high hydrophobicity, they participated in the adsorption process onto the MS surface,

through a synergetic effect that caused corrosion inhibition [29-32]. CP seems to be a great inhibitor in 0.5 M H<sub>2</sub>OS<sub>4</sub>, and its potential was enhanced by KI, since it achieved 98.8(%) IE(%). Similar outcomes have been reported in literature [33, 34].

### Adsorption isotherm

θ parameters determined from EIS measurements are listed in Table 1, and they were used to identify the best adsorption isotherm. Ec measurements confirmed the best fitted Langmuir's adsorption isotherm, for which the following relation has been used [35]:

$$\frac{C}{\theta} = \frac{1}{K_{ads}} + C \quad (4)$$

Fig. 5 shows that the plot between C/θ and C of CP and CP + KI in 0.5 M H<sub>2</sub>OS<sub>4</sub>, at 308 K, gave a straight line.

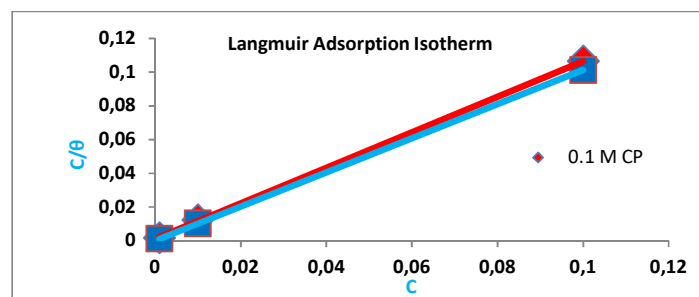


**Figure 5:** Langmuir's adsorption isotherm for CP and CP + KI in H<sub>2</sub>SO<sub>4</sub>.

It is evident from the outcomes that linear R<sup>2</sup> was 1, which implies that the adsorption mechanism of CP and CP + KI molecules onto the MS surface obeyed Langmuir's isotherm [36] (Table 2).

**Table 2:** Karl Pearson's coefficient of CP and CP + KI adsorption isotherm in 0.5 M H<sub>2</sub>SO<sub>4</sub>.

Organic inhibitor	Adsorption isotherm	R2
CP	Langmuir's	0.9999
CP + KI	Langmuir's	1

Standard ΔG<sub>ads</sub> of CP and CP + KI is related to K<sub>ads</sub>, and it can be evaluated by the following equation [37]:

$$\Delta G_{ads}^0 = -RT \ln(55.5K_{ads}) \quad (5)$$

where R is the universal gas constant and 55.5 is molar C of H<sub>2</sub>O. As shown in Table 3, CP and CP + KI ΔG<sub>ads</sub> values were negative (-27.97 and -34.13 kJ/mol, respectively), which indicates that their adsorption onto the MS surface was a spontaneous process that occurred through a chemical bond (chemisorption) [38].

**Table 3:** Adsorption parameters for MS surface corrosion in H<sub>2</sub>SO<sub>4</sub> with inhibitors, at 308 K.

Inhibitor	Intercept	K (L/mol)	$\Delta G_{ads}^0$ (kJ/mol)
CP	$1 \times 10^{-3}$	1000	-27.97
CP + KI	$9 \times 10^{-5}$	11,111.1	-34.13

### SEM

SEM images of MS specimens after immersion in H<sub>2</sub>SO<sub>4</sub> with 10<sup>-1</sup> M CP and CP + KI, show a smoother surface (Fig. 6a and b). This is because the inhibitor molecules hindered MS dissolution process, by developing a barrier layer on its surface, which retarded the corrosion process.

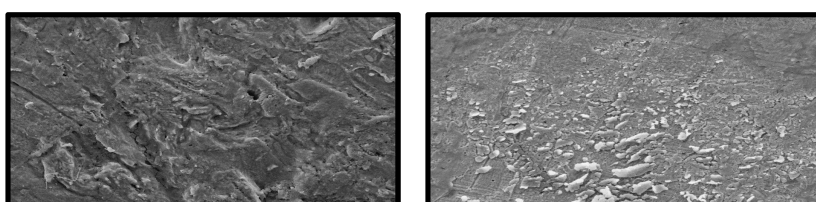


**Figure 6:** SEM images of the MS surface in 0.5 M H<sub>2</sub>SO<sub>4</sub> with: (a) 10<sup>-1</sup> M CP; and (b) 10<sup>-1</sup> M CP + KI (magnification × 2000).

Hence, CP protected MS against corrosion in H<sub>2</sub>SO<sub>4</sub> solutions. In addition, from the images, one also concludes that I<sup>-</sup> ions played an important role in CI, through their participation in the adsorption process, which enhanced MS protection [39, 40].

### AFM

Fig. 7(a) shows that, upon CP addition to H<sub>2</sub>SO<sub>4</sub>, some small, even and compact particles, which orderly scattered on the MS surface, covered it almost completely.

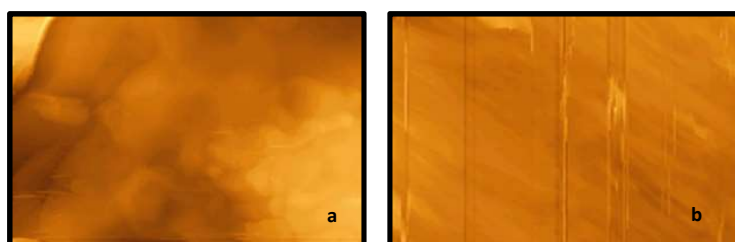


**Figure 7:** Two-dimensional AFM images of the MS surface in 10<sup>-1</sup> M: (a) CP; and (b) CP + KI.

On the other hand, AFM image in Fig. 7b shows that, with CP + KI, the MS surface became more flat, uniform and homogeneous, which reveals that the inhibitor offered an appreciable resistance to corrosion, due to I<sup>-</sup> synergetic effect.

The MS surface  $\eta$  in blank H<sub>2</sub>SO<sub>4</sub> was up to 1102.8 nm, while it decreased to 392.9 nm upon CP addition, and was further reduced to 259 nm with CP + KI ( Table 4).

**Table 4:** MS  $\eta$  from AFM.

Compound	Average area $\eta$
CP	392.9
CP+KI	259.0
H <sub>2</sub> SO <sub>4</sub>	1102.8

Similar results were reported in literature for organic inhibitors in acidic media [41, 42]. Therefore, MS CI took place due to the formation of a protective layer by CP and CP + KI, through the adsorption of their molecules onto the alloy surface. The three-dimensional AFM images of the MS surface, in H<sub>2</sub>SO<sub>4</sub> with CP and CP + KI, are shown in Fig. 8a and b.

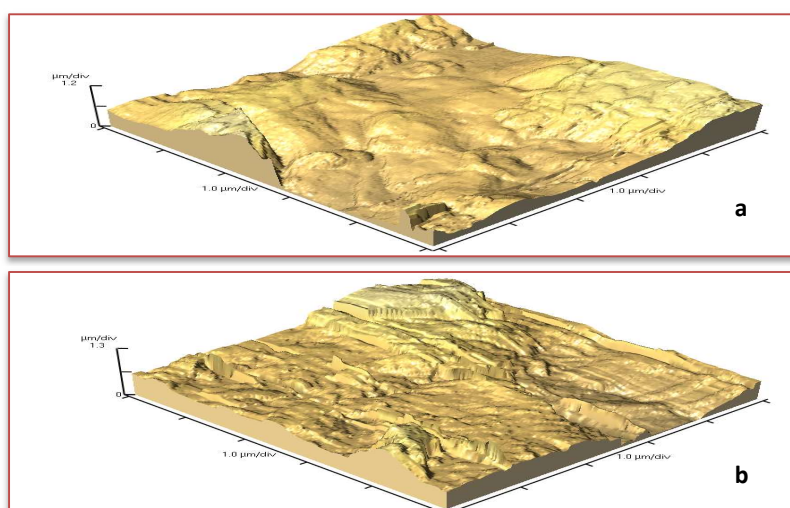


**Figure 8:** Three-dimensional AFM images of the MS surface in 10<sup>-1</sup> M: (a) CP; and (b) CP + KI.

## Conclusion

The outcomes of the present work revealed that the studied inhibitors are indeed very promising, with excellent ability to hinder MS corrosion process in H<sub>2</sub>SO<sub>4</sub>. EIS results showed that, upon the addition of CP and CP + KI to H<sub>2</sub>SO<sub>4</sub>, the protective film developed on the metal/electrolyte interface caused an increase in  $R_{ct}$ , and a decrease in  $C_{dl}$ . It was also confirmed that the inhibition mechanism was linked to CP and CP + KI adsorption, which obeys Langmuir's isotherm. The values from SM  $\eta$  studies in the solution with inhibitor were much lower than those in the blank one. This means that CP and CP + KI are effective organic CI.

## Acknowledgements

The authors thank USIC, DU for providing characterization facilities.

## Competing financial interests

The authors declare no competing financial interests.



### **Author's contributions**

**Neelu Dheer:** was in main charge of this research, having performed experiments and analyzed experimental data; discussed results and helped analyzing them. **Amarpreet K. Kalra:** was in main charge of this research, having performed experiments and analyzed experimental data. **Darshan Singh:** discussed results and helped analyzing them. **Sanjeev Kumar Ujjain:** edited the paper. **Preety Ahuja:** edited the paper. **Gurmeet Singh:** reviewed and edited the paper. **M. Ramananda Singh:** conceived the idea and supervised the whole project; prepared the paper. **Rajni Kanojia:** conceived the idea and supervised the whole project; prepared the paper; edited the paper.

### **Abbreviations**

**AC:** alternating current  
**AFM:** atomic force microscope  
**C:** concentration  
**C<sub>dl</sub>:** double layer capacitance  
**CI:** corrosion inhibitor/inhibition  
**CP:** 3-carboxypyridine  
**Ec:** electrochemical  
**EIS:** electrochemical impedance spectroscopy  
**H<sub>2</sub>SO<sub>4</sub>:** sulphuric acid  
**IE(%):** inhibition efficiency  
**K<sub>ads</sub>:** adsorption equilibrium constant  
**KI:** potassium iodide  
**Log C:** logarithm concentration  
**MS:** mild steel  
**OCP:** open circuit potential  
**R<sup>2</sup>:** correlation coefficient  
**R<sub>ct</sub>:** charge transfer resistance  
**R<sub>p</sub>:** polarization resistance  
**SEM:** scanning electron microscopy  
**SM:** surface methodology  
**T:** temperature  
**WE:** working electrode

### **Symbols definition**

**ΔG<sub>ads</sub>:** adsorption free energy  
**η:** surface roughness  
**θ:** degree of surface coverage  
**θ<sub>max</sub>:** phase angle

### **References**

1. Ehteram AN. Evaluation of inhibitive action of some quaternary N-heterocyclic compounds on the corrosion of Al-Cu alloy in hydrochloric acid. *Mater Chem Phys.* 2009;(2-3):114:533-541. <https://doi.org/10.1016/j.matchemphys.2008.09.065>

2. Mahmoud AB. The effect of structure parameters on the corrosion inhibition effect of some heterocyclic nitrogen organic compounds. *J Mol Liq.* 2016;219:128-141. <https://doi.org/10.1016/j.molliq.2016.03.012>
3. Arumugam R, Panneerselvam A, Sadhasivam G. Structural and electronic impacts on corrosion inhibition activity of novel heterocyclic carboxamides derivatives on mild steel in 1 M HCl environment: Experimental and theoretical approaches. *J Mol Liq.* 2022;359:119218. <https://doi.org/10.1016/j.molliq.2022.119218>
4. Dileep KY, Mumtaz AQ. Electrochemical investigation of Substituted Pyranopyrazoles Adsorption on Mild Steel in Acid Solution. *Ind Eng Chem Res.* 2012;(51)24:8194-8210. <https://doi.org/10.1021/ie3002155>
5. Sudheer, Mumtaz AQ. 2-Amino-3,5-dicarbonitrile-6-thio-pyridines: New and Effective Corrosion Inhibitors for Mild Steel in 1 M HCl. *Ind Eng Chem Res.* 2014;(53)8:2851-2859. <https://doi.org/10.1021/ie401633y>
6. Priyanka S, Madhan K, Mumtaz AQ et al. Bispyranopyrazoles as Green Corrosion Inhibitors for Mild Steel in Hydrochloric Acid: Experimental and Theoretical Approach. *ACS Omega.* 2018;(3)9:11151-11162. <https://doi.org/10.1021/acsomega.8b01300>
7. Priyanka S, Eno EE, Lukman OO et al. Electrochemical, Theoretical, and Surface Morphological Studies of Corrosion Inhibition Effect of Green Naphthyridine Derivatives on Mild Steel in Hydrochloric Acid. *J Phys Chem C.* 2016;(120)6:3408-3419. <https://doi.org/10.1021/acs.jpcc.5b11901>
8. Chandrabhan V, Kyong YR, Mumtaz AQ et al. Pyridine based N-heterocyclic compounds as aqueous phase corrosion inhibitors: A review. *J Taiwan Inst Chem Eng.* 2020;117:265-277. <https://doi.org/10.1016/j.jtice.2020.12.011>
9. Humira A, Ashish K. Understanding functional group effect on corrosion inhibition efficiency of selected organic compounds. *J Mol Liq.* 2021;344:117755. <https://doi.org/10.1016/j.molliq.2021.117755>
10. McCafferty E, Norman H. Double layer capacitance of iron and corrosion inhibition with polymethylene diamines. *J Electrochem Soc.* 1972;(2)119:146-154. <https://doi.org/10.1149/1.2404150>
11. Emeka EO, Ying L, Fiona HW. Corrosion inhibition and adsorption behavior of methionine on mild steel in sulfuric acid and synergistic effect of iodide ion. *J Col Interf Sci.* 2007;(310)1:90-98. <https://doi.org/10.1016/j.jcis.2007.01.038>
12. Yurii IK. Organic inhibitors of corrosion of metals. New York. Plenum. 1996. <https://doi.org/10.1007/978-1-4899-1956-4>
13. Fernando SDS, Almir S. Caffeic acid as green corrosion inhibitors for mild steel. *Corros Sci.* 2009;(51)3:642-649. <https://doi.org/10.1016/j.corsci.2008.12.013>
14. Jia W, Jinyan L, Qian L et al. The inhibition performance of heterocyclic compounds on Q235 steel in methanol/formic acid medium: Experimental and theory. *J Mol Liq.* 2021;343:117663. <https://doi.org/10.1016/j.molliq.2021.117663>
15. Mourad F, Yassine L, Yassine K et al. Electrochemical and theoretical studies on the corrosion inhibition performance of some synthesized d-Limonene based heterocyclic compounds. *J Mol Struct.* 2021;1244:130957. <https://doi.org/10.1016/j.molstruc.2021.130957>
16. Mohammad S, Vandana S, Dheeraj SC et al. Chromeno naphthyridines based heterocyclic compounds as novel acidizing corrosion inhibitors: Experimental, surface and computational study. *J Mol Liq.* 2021;322:114825. <https://doi.org/10.1016/j.molliq.2020.114825>

17. Anees AK, Ahmed NA, Nagham AA et al. Combined influence of iodide ions and *Xanthium Strumarium* leaves extract as eco-friendly corrosion inhibitor for low-carbon steel in hydrochloric acid. *Curr Res Green Sust Chem.* 2022;5:100278. <https://doi.org/10.1016/j.crgsc.2022.100278>
18. Eliazar AT, Rosa LCM, Evelin G et al. The influence of iodide in corrosion inhibition by organic compounds on carbon steel: Theoretical and experimental studies. *Appl Surf Sci.* 2020;514:145928. <https://doi.org/10.1016/j.apsusc.2020.145928>
19. Shveta S, Sourav KS, Namhyun K et al. Multidimensional analysis for corrosion inhibition by Isoxsuprine on mild steel in acidic environment: Experimental and computational approach. *J Mol Liq.* 2022;357:119129. <https://doi.org/10.1016/j.molliq.2022.119129>
20. Xiao-Long L, Bin X, Chuan L et al. Adsorption and corrosion inhibition performance of two planar rigid pyridinecarboxaldehyde-based double Schiff bases for mild steel in HCl solution: Experimental and computational investigations. *J Mol Liq.* 2022;355:118926. <https://doi.org/10.1016/j.molliq.2022.118926>
21. Abdullah S, Handan Y, Ramazan S. Experimental studies on the corrosion inhibition performance of 2-(2-aminophenyl)benzimidazole for mild steel protection in HCl solution. *J Taiwan Inst Chem Eng.* 2022;134:104349. <https://doi.org/10.1016/j.jtice.2022.104349>
22. Sanja M, Ivica S. Thermodynamic characterization of metal dissolution and inhibitor adsorption processes in the low carbon steel/mimosa tannin/ sulphuric acid system. *Appl Surf Sci.* 2002;(199)1-4:83-89. [https://doi.org/10.1016/S0169-4332\(02\)00546-9](https://doi.org/10.1016/S0169-4332(02)00546-9)
23. Neelu D, Rajni K, Gurmeet S et al. 4(2-Pyridylazo) Resorcinol as Effective Corrosion Inhibitor for Mild Steel in 0.5 M H<sub>2</sub>SO<sub>4</sub>. *Surf. Eng.* 2007;23(3):187-193. <https://doi.org/10.1179/174329407X174470>
24. Asha T, Jeeja RAT, Abraham J. Extended protection of mild steel in molar HCl using the *Garcinia indica* fruit and iodide ions, electrochemical, thermodynamic and kinetic studies. *J Ind Chem Soc.* 2021;(98)10:100167. <https://doi.org/10.1016/j.jics.2021.100167>
25. Dheeraj SC, Mumtaz AQ, Tawfik AS et al. Bis(2-aminoethyl)amine-modified graphene oxide nanoemulsion for carbon steel protection in 15% HCl: effect of temperature and synergism with iodide ions. *J Coll Interf Sci.* 2020;564:124-133. <https://doi.org/10.1016/j.jcis.2019.12.125>
26. Mukerrem S, Semra B, Hamza Y. The inhibition effects of some cyclic nitrogen compounds on the corrosion of the steel in NaCl mediums. *Appl Surf Sci.* 2002;195:1-7. [https://doi.org/10.1016/S0169-4332\(01\)00783-8](https://doi.org/10.1016/S0169-4332(01)00783-8)
27. Hassane L, Abdel KC, Maryam C et al. Evaluating the corrosion inhibition properties of novel 1,2,3-triazolyl nucleosides and their synergistic effect with iodide ions against mild steel corrosion in HCl: A combined experimental and computational exploration. *J Mol Liq.* 2021;338:116522. <https://doi.org/10.1016/j.molliq.2021.116522>
28. Weiwei Z, Hui-Jing L, Ankai W et al. Synergistic inhibition effect of N-(furan-2-ylmethyl)-7H-purin-6-amine and iodide ion for mild steel corrosion in 1 mol/L HCl. *Mater Corros.* 2019;(71)3:498-507. <https://doi.org/10.1002/maco.201911146>
29. Xianghong L, Shuduan D. Synergistic inhibition effect of walnut green husk extract and potassium iodide on the corrosion of cold rolled steel in Trichloroacetic acid solution. *J Mater Res Technol.* 2020;(9)6:15604-15620. <https://doi.org/10.1016/j.jmrt.2020.11.018>

30. Lamia B, Mousa AN, Djamel D et al. Synthesis, characterization and the inhibition activity of 3-(4-cyanophenylazo)-2,4-pentanedione (L) on the corrosion of carbon steel: synergistic effect with other halide ions in 0.5 M H<sub>2</sub>SO<sub>4</sub>. *J Mol Struct.* 2019;1177:371-380. <https://doi.org/10.1016/j.molstruc.2018.09.079>
31. Eliazar AT, Rosa LCM, Evelin G et al. The influence of iodide in corrosion inhibition by organic compounds on carbon steel: theoretical and experimental studies. *Appl Surf Sci.* 2020;514:145928. <https://doi.org/10.1016/j.apsusc.2020.145928>
32. Rajni K, Gurmeet S. An interesting and efficient organic corrosion inhibitor for mild steel in acidic medium. *Surf Eng.* 2005;21:180-186. <https://doi.org/10.1179/174329405X49985>
33. Roland TL, Olukeye T. Corrosion inhibition properties of the synergistic effect of 4-hydroxy-3-methoxybenzaldehyde and hexadecyltrimethylammoniumbromide on mild steel in dilute acid solutions. *J King Saud Univ Eng Sci.* 2018;30(4):384-390. <https://doi.org/10.1016/j.jksues.2016.10.001>
34. Revathi M, Abraham J et al. Adsorption and electrochemical studies on the synergistic interaction of alkyl benzimidazoles and ethylene thiourea pair on mild steel in hydrochloric acid. *J Taiwan Inst Chem Eng.* 2014;45(6):3021-3032. <https://doi.org/10.1016/j.jtice.2014.08.033>
35. Xianghong L, Shuduan D, Guannan M et al. Inhibition effect of nonionic surfactant on the corrosion of cold rolled steel in hydrochloric acid. *Corros Sci.* 2008;50:420-430. <https://doi.org/10.1016/j.corsci.2007.08.014>
36. Djamel D, Tahar D, Hanane H et al. Corrosion inhibition of mild steel by two new S-heterocyclic compounds in 1 M HCl: Experimental and computational study. *Corros Sci.* 2015;94:21-37. <https://doi.org/10.1016/j.corsci.2015.01.025>
37. Siham EA, Khalid K, Avni B et al. New pyrazole derivatives as effective corrosion inhibitors on steel-T electrolyte interface in 1 M HCl: Electrochemical, surface morphological (SEM) and computational analysis. *Col Surf A.* 2020;604:125325. <https://doi.org/10.1016/j.colsurfa.2020.125325>
38. Zeinab RF, Moustapha EM, El Hassane A et al. The inhibition tendencies of novel hydrazide derivatives on the corrosion behavior of mild steel in hydrochloric acid solution. *J Mat Res Technol.* 2022;16:1422-1434. <https://doi.org/10.1016/j.jmrt.2021.12.035>
39. Ambrish S, Yuanhua L, Songsong C et al. Electrochemical and surface studies of some porphines as corrosion inhibitor for J55 steel in sweet corrosion environment. *Appl Surf Sci.* 2015;359:331-339. <https://doi.org/10.1016/j.apsusc.2015.10.129>
40. Heba EH, Ahmed AF, Eslam AM et al. Experimental and theoretical assessment of benzopyran compounds as inhibitors to steel corrosion in aggressive acid solution. *J Mol Struct.* 2022;1249:131641. <https://doi.org/10.1016/j.molstruc.2021.131641>
41. Khalid AA, Ruby A, Ajahar K et al. Evaluation of corrosion inhibition performance of thiazolidine-2,4-diones and its amino derivative: Gravimetric, electrochemical, spectroscopic, and surface morphological studies. *Process Saf Environ Prot.* 2022;159:178-197. <https://doi.org/10.1016/j.psep.2021.12.061>
42. Xianghong L, Shuduan D, Hui F et al. Synergism between rare earth cerium (IV) ion and vanillin on the corrosion of steel in H<sub>2</sub>SO<sub>4</sub> solution: weight loss, electrochemical, UV-vis, FTIR, XPS and AFM approaches. *Appl Surf Sci.* 2008;(254)17:5574-5586. <https://doi.org/10.1016/j.apsusc.2008.03.026>